Supplementary Tables:

Table 1: Definition of relevant optical and acoustic measurement parameters in biophotonic imaging.

	Parameter	Symbol	Unit	Definition	Average value in soft tissue*	Ref
Optical	Optical absorption coefficient	μ_a	cm^{-1}	Probability of photon absorption per unit length travelled by the photon	0.1 - 0.5	[1,2]
	Refractive index	n	-	Ratio of the velocity of light in a vacuum to the velocity of light in a medium	1.33 - 1.51	[1,2]
	Anisotropy factor	g	-	Represents the effects of directionally dependent scattering	0.7 - 0.9	[1,2]
	Reduced scattering coefficient	μ_s'	cm^{-1}	Probability of photon scattering per unit length travelled by the photon	10-20	[1,2]
Acoustic	Acoustic attenuation coefficent	α	$dB \cdot cm^{-1} \cdot MHz^{-1}$	Extent of reduction of an acoustic wave when propagating within a medium	0.1-1.6	[3,4]
	Speed of sound	c	$m \cdot s^{-1}$	Velocity of acoustic wave propagation within a medium	1450 - 1730	[3,4]
	Backscattering coefficient	μ_{bs}	$m^{-1}sr^{-1}$	Differential scattering cross section per unit volume at a scattering angle of 180°	3.5×10^{-4}- 9×10^{-4}	[4,5]
Thermoelastic	Grüneisen Parameter	Γ	-	Measure of thermoelastic efficiency	0.25 -0.9	[6]
Fluorescence	Emission spectrum	$I_e(\lambda)$	nm	Wavelength-dependent fluorescent output spectrum	**	
	Emission quantum yield	φ_{QY}	%	Measure of photon emission efficiency defined by the ratio of the number of photons emitted to the number of photons absorbed	**	
	Emission lifetime	τ	ns	Time a fluorophore spends in the excited state before returning to the ground state by photon emission	**	

Notes: *These are just representative values. For more accurate numbers see literature. Speed of sound can vary with temperature.

**Depending on fluorophore

Table 2: Relevant optical and acoustic parameters of different materials without the use of additives. Optical properties refer to a wavelength range of 600 – 900 nm.

	Optical				Acoustic		
Material	**Intrinsic μ_a (cm^{-1})**	**Intrinsic μ_s' (cm^{-1})**	**Refr. index**	**Ref.**	**c ($m \cdot s^{-1}$)**	**($dB \cdot cm^{-1}$) at frequency (MHz)**	**Ref.**
General soft tissue	0.1-0.5	10-20	1.33-1.51	[2]	1450–1730	0.1–1.6 $dB \cdot cm^{-1} \cdot MHz^{-1}$	[3,4]
Aqueous suspension	negligible*	negligible	1.34	[7]	1480-1574	0.0022 at 1 MHz	[3]
Agar/Gelatin	negligible	negligible	1.35	[8]	1490-1650	0.1–1.5 $dB \cdot cm^{-1} \cdot MHz^{-1}$	[9–16]
Polyacrylamide (10%-20%)	negligible	negligible	1.35	[17]	1540-1590	0.08-0.14 at 1 MHz 0.7 at 5 MHz	[11,18]
PVA	Dedependent on preparation**	Dedependent on preparation**	1.35	[19,20]	1510-1570	0.075–0.56 $dB \cdot cm^{-1} \cdot MHz^{-1}$	[11,21–23]
Co-polymer in oil	negligible (dependent on polymer)	negligible (dependent on polymer)	1.47	[24]	1420-1500	0.4-7 at 3.5 MHz	[25–27]
PVCP (including 0 - 90% softener)	negligible	negligible	1.52	[28]	1350-1580	0.6-0.9 at 1 MHz 1-30 at 4 MHz 6.45-8.24 at 5 MHz	[28–34]
Silicone	negligible	negligible	1.4	[35]	970-1200	1.8 at 3 MHz 14.0 at 5 MHz 14.7 at 7 MHz	[11,36–38]
Polyurethane	negligible	negligible	1.5	[39]	1400-1470	0.5–0.7 $dB \cdot cm^{-1} \cdot MHz^{-1}$	[38,40]
Polyester, Epoxy resin	negligible	negligible	1.54	[41–43]	1844-3118	7–17 at 0.5 MHz	[44]

**Absorption spectra of water can be obtained from Hale and Querry et al.*[45]

*** dependent on the number, length and rate of freeze and thaw cycles, by the grade of the PVA (molecular weight, degree of saponification) and its concentration in the aqueous solution, by the presence of additives and by the type of solvent*[23,46–50]

Table 3: Overview of types of heterogeneous phantoms used in biophotonics. Static implementations are targeted for applications requiring constant properties (e.g. breast tumour), whilst dynamic implementations focus on applications requiring time-varying properties (e.g. brain activation). If the material of embedded inclusions or targets differs from the base material, mismatches in optical properties (e.g. refractive index) or acoustic impedance can be introduced potentially leading to imaging artefacts.

Base	Advantages	Disadvantages	Target	Implementations	
				Static	Dynamic
Liquid	+ Reliable adjustment of optical properties + Movement / replacement of inclusion possible + High homogeneity + Simple preparation + Simple change of optical properties	- Container walls can create light-guiding effects/acoustic boundaries[51–53] - Poor stability over time - Complex to handle/transport - Acoustic / mechanical parameters cannot sufficiently be mimicked - Low architectural flexibility	Liquid 	- Liquid inclusions of contrasting optical properties in homogeneous medium[54] - Layers of different optical properties[55,56]	- Flow through sphere[57] or tube[58] to mimic dye bolus
			Solid 	- targets of contrasting optical properties[53,59–62]	
Solid	+ Good stability + No containing vessel needed + Simple maintenance + High architectural flexibility (e.g. 3D-shape, layered structures)	- Difficult to change properties / position of the inclusion - Hardener may change the inclusion properties[63] - Fabrication may be challenging	Liquid 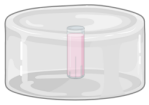	- Liquid inclusions of contrasting optical properties[64]	- Perfused channel-arrays[65] or tubings[66] - Solid layer on top of a homogenous liquid medium with variable haemoglobin oxygenation[56,67,68]
			Solid 	- Targets of contrasting optical properties (e.g. fibers, spheres)[53,63] - Layers of different optical properties[69–71]	- Targets mimicking local absorption changes by electrochromic[72], thermochromic[73–75], or mechanical methods[77] - Layers of different optical properties with mechanical movement[76]

Table 4: Materials used for direct 3D-printing of optical imaging phantoms.

Material		Absorber	Scatterer	Printing method	Ref
Hydrogels (e.g. gelatin, agar)		Molecular dyes, Coffee	TiO_2	Fused deposition modeling	[79,80]
Copolymer-in-oil		Graphite powder	TiO_2	Fused deposition modeling	[24,81]
Acrylonitrile butadiene styrene (ABS)		Nigrosin[82]	TiO_2[82]	(dual extrusion) fused deposition modeling	[82–84]
Polylactid acid (PLA)		-	-	(dual extrusion) fused deposition modeling	[85]
Commercial photopolymer	Vero-series (Stratasys Inc., Eden Prairie, MN)	Veroblack (containing black pigments)	Verowhite (containing TiO_2)	PolyJet	[86–88]
	Tango-Series, Stratasys Inc., Eden Prairie, MN)	TangoBlack (containing black pigments)			[89]
	Methacrylate based photopolymers (e.g. Formlabs series, Somerville, Massachusetts; E-Shell series, EnvisionTec, Germany)	Commercial colour pigments, Black ink, molecular dye (e.g. Projet 900NP)	polystyrene microspheres, TiO_2	Stereolithography	[90–93]

Bibliography

1. Bigio IJ, Fantini S. *Quantitative Biomedical Optics*. Cambridge University Press; 2016. doi:10.1017/cbo9781139029797

2. Jacques SL. Optical properties of biological tissues: a review. *Phys Med Biol*. 2013;58(11):R37-R61. doi:10.1088/0031-9155/58/11/R37

3. Azhari H. Appendix A: Typical Acoustic Properties of Tissues. In: *Basics of Biomedical Ultrasound for Engineers*. John Wiley & Sons, Inc.; 2010:313-314. doi:10.1002/9780470561478.app1

4. Collins DE. ICRU REPORT 61: Tissue substitutes, phantoms and computational modelling in medical ultrasound. *Radiol Technol*. 1999;71(2):215-215. Accessed June 25, 2020. https://go.gale.com/ps/i.do?p=HRCA&sw=w&issn=00338397&v=2.1&it=r&id=GALE%7CA57827691&sid=googleScholar&linkaccess=fulltext

5. Nicholas D. Evaluation of backscattering coefficients for excised human tissues: results, interpretation and associated measurements. *Ultrasound Med Biol*. 1982;8(1):17-28. doi:10.1016/0301-5629(82)90065-5

6. Grüneisen E. Theorie des festen Zustandes einatomiger Elemente. *Ann Phys*. 1912;344(12):257-306. doi:10.1002/andp.19123441202

7. Linford J, Shalev S, Bews J, Brown R, Schipper H. Development of a tissue-equivalent phantom for diaphanography. *Med Phys*. 1986;13(6):869-875. doi:10.1118/1.595948

8. Durkin AJ, Jaikumar S, Richards-Kortum R. Optically Dilute, Absorbing, and Turbid Phantoms for Fluorescence Spectroscopy of Homogeneous and Inhomogeneous Samples. *Appl Spectrosc*. 1993;47(12):2114-2121. doi:10.1366/0003702934066244

9. Bush NL, Hill CR. Gelatine-alginate complex gel: A new acoustically tissue-equivalent material. *Ultrasound Med Biol*. 1983;9(5):479-484. doi:10.1016/0301-5629(83)90020-0

10. Madsen EL, Zagzebski JA, Banjavie RA, Jutila RE. Tissue mimicking materials for ultrasound phantoms. *Med Phys*. 1978;5(5):391-394. doi:10.1118/1.594483

11. Zell K, Sperl JI, Vogel MW, Niessner R, Haisch C. Acoustical properties of selected tissue phantom materials for ultrasound imaging. *Phys Med Biol*. 2007;52(20). doi:10.1088/0031-9155/52/20/N02

12. Madsen EL, Frank GR, Dong F. Liquid or solid ultrasonically tissue-mimicking materials with very low scatter. *Ultrasound Med Biol*. 1998;24(4):535-542. doi:10.1016/S0301-5629(98)00013-1

13. Burlew MM, Madsen EL, Zagzebski JA, Banjavic RA, Sum SW. A new ultrasound tissue-equivalent material. *Radiology*. 1980;134(2):517-520. doi:10.1148/radiology.134.2.7352242

14. Rajagopal S, Sadhoo N, Zeqiri B. Reference Characterisation of Sound Speed and Attenuation of the IEC Agar-Based Tissue-Mimicking Material Up to a Frequency of 60MHz. *Ultrasound Med Biol*. 2015;41(1):317-333. doi:10.1016/j.ultrasmedbio.2014.04.018

15. IEC. *IEC 60601-2-37:2007 Particular Requirements for the Basic Safety and Essential Performance of Ultrasonic Medical Diagnostic and Monitoring Equipment*.; 2007. https://webstore.iec.ch/publication/2652

16. Cournane S, Fagan AJ, Browne JE. Review of ultrasound elastography quality control

and training test phantoms. *Ultrasound*. 2012;20(1):16-23. doi:10.1258/ult.2011.011033

17. McDonald MJ, Turci SM, Bunn HF, Garrick LM, Garrick MD, Brewer GJ. Structural and functional studies of hemolysates from genetically selected high and low level DPG rat strains. *Prog Clin Biol Res*. 1981;55:215-224.

18. Prokop AF, Vaezy S, Noble ML, Kaczkowski PJ, Martin RW, Crum LA. Polyacrylamide gel as an acoustic coupling medium for focused ultrasound therapy. *Ultrasound Med Biol*. 2003;29(9):1351-1358. doi:10.1016/S0301-5629(03)00979-7

19. Yokoyama F, Masada I, Shimamura K, Ikawa T, Monobe K. Morphology and structure of highly elastic poly(vinyl alcohol) hydrogel prepared by repeated freezing-and-melting. *Colloid Polym Sci*. 1986;264(7):595-601. doi:10.1007/BF01412597

20. Yamaura K, Itoh M, Tanigami T, Matsuzawa S. Properties of gels obtained by freezing/thawing of poly(vinyl alcohol)/water/dimethyl sulfoxide solutions. *J Appl Polym Sci*. 1989;37(9):2709-2718. doi:10.1002/app.1989.070370921

21. Kharine A, Manohar S, Seeton R, et al. Poly(vinyl alcohol) gels for use as tissue phantoms in photoacoustic mammography. 2003;48(3):357-370. doi:10.1088/0031-9155/48/3/306

22. Malone AJ, Cournane S, Naydenova IG, Fagan AJ, Browne JE. Polyvinyl alcohol cryogel based vessel mimicking material for modelling the progression of atherosclerosis. *Phys Medica*. 2020;69:1-8. doi:10.1016/j.ejmp.2019.11.012

23. Surry KJM, Austin HJB, Fenster A, Peters TM. Poly(vinyl alcohol) cryogel phantoms for use in ultrasound and MR imaging. *Phys Med Biol*. 2004;49(24):5529-5546. doi:10.1088/0031-9155/49/24/009

24. Dong E, Zhao Z, Wang M, et al. Three-dimensional fuse deposition modeling of tissue-simulating phantom for biomedical optical imaging. *J Biomed Opt*. 2015;20(12):121311. doi:10.1117/1.JBO.20.12.121311

25. Cabrelli LC, Pelissari PIBGB, Deana AM, et al. Stable phantom materials for ultrasound and optical imaging. *Phys Med Biol*. 2017;62(2):432-447. doi:10.1088/1361-6560/62/2/432

26. Oudry J, Bastard C, Miette V, Willinger R, Sandrin L. Copolymer-in-oil phantom materials for elastography. *Ultrasound Med Biol*. 2009;35(7):1185-1197. doi:10.1016/j.ultrasmedbio.2009.01.012

27. Cabrelli LC, Grillo FW, Sampaio DRT, Carneiro AAO, Pavan TZ. Acoustic and Elastic Properties of Glycerol in Oil-Based Gel Phantoms. *Ultrasound Med Biol*. 2017;43(9):2086-2094. doi:10.1016/j.ultrasmedbio.2017.05.010

28. Vogt WC, Jia C, Wear KA, Garra BS, Joshua Pfefer T. Biologically relevant photoacoustic imaging phantoms with tunable optical and acoustic properties. *J Biomed Opt*. 2016;21(10):101405. doi:10.1117/1.JBO.21.10.101405

29. Fonseca M, Zeqiri B, Beard PC, Cox BT. Characterisation of a phantom for multiwavelength quantitative photoacoustic imaging. *Phys Med Biol*. 2016;61(13):4950-4973. doi:10.1088/0031-9155/61/13/4950

30. Spirou G, Oraevsky A, Vitkin I, Whelan W. Optical and acoustic properties at 1064 nm of polyvinyl chloride-plastisol for use as a tissue phantom in biomedical optoacoustics. *Phys Med Biol*. 2005;50.

31. Bakaric M, Miloro P, Zeqiri B, Cox BT, Treeby BE. The Effect of Curing Temperature and Time on the Acoustic and Optical Properties of PVCP. *IEEE Trans Ultrason*

Ferroelectr Freq Control. 2020;67(3):505-512. doi:10.1109/TUFFC.2019.2947341

32. Madsen EL, Frank GR, Krouskop TA, Varghese T, Kallel F, Ophir J. Tissue-mimicking oil-in-gelatin dispersions for use in heterogeneous elastography phantoms. *Ultrason Imaging*. 2003;25(1):17-38. doi:10.1177/016173460302500102

33. Bohndiek SE, Bodapati S, Van De Sompel D, Kothapalli S-RR, Gambhir SS. Development and Application of Stable Phantoms for the Evaluation of Photoacoustic Imaging Instruments. Brody JP, ed. *PLoS One*. 2013;8(9):1-14. doi:10.1371/journal.pone.0075533

34. Hungr N, Long JJ-AA, Beix V, Troccaz J. A realistic deformable prostate phantom for multimodal imaging and needle-insertion procedures. 2012;39(4):2031-2041. doi:10.1118/1.3692179

35. Lualdi M, Colombo A, Farina B, Tomatis S, Marchesini R. A phantom with tissue-like optical properties in the visible and near infrared for use in photomedicine. *Lasers Surg Med*. 2001;28(3):237-243. doi:10.1002/lsm.1044

36. Wilson DJ, Ridgway JP, Evans A. *Clinical Physics and Physiological Measurement To Cite This Article: J Robertson et Al*. Vol 13.; 1992.

37. - Document - ICRU REPORT 61: TISSUE SUBSTITUTES, PHANTOMS AND COMPUTATIONAL MODELLING IN MEDICAL ULTRASOUND. Accessed April 18, 2020. https://go.gale.com/ps/anonymous?id=GALE%7CA57827691&sid=googleScholar&v=2.1&it=r&linkaccess=abs&issn=00338397&p=AONE&sw=w

38. Cafarelli A, Miloro P, Verbeni A, Carbone M, Menciassi A. Speed of sound in rubber-based materials for ultrasonic phantoms. *J Ultrasound*. 2016;19(4):251-256. doi:10.1007/s40477-016-0204-7

39. Vernon ML, Fréchette J, Painchaud Y, Caron S, Beaudry P. Fabrication and characterization of a solid polyurethane phantom for optical imaging through scattering media. *Appl Opt*. 1999;38(19):4247. doi:10.1364/ao.38.004247

40. Cournane S, Cannon L, Browne JE, Fagan AJ. Assessment of the accuracy of an ultrasound elastography liver scanning system using a PVA-cryogel phantom with optimal acoustic and mechanical properties. *Phys Med Biol*. 2010;55(19):5965-5983. doi:10.1088/0031-9155/55/19/022

41. Firbank M, Oda M, Delpy DT, Firbankt M, Odq M, Delpyt DT. An improved design for a stable and reproducible phantom material for use in near-infrared spectroscopy and imaging. *Phys Med Biol*. 1995;40(5):955-961. doi:10.1088/0031-9155/40/5/016

42. Firbank M, Delpy DT. A phantom for the testing and calibration of near infra-red spectrometers. *Phys Med Biol*. 1994;39(9):1509-1513. doi:10.1088/0031-9155/39/9/015

43. Sukowski U, Schubert F, Grosenick D, Rinneberg H. Preparation of solid phantoms with defined scattering and absorption properties for optical tomography. *Phys Med Biol*. 1996;41(9):1823-1844. doi:10.1088/0031-9155/41/9/017

44. Clarke AJ, Evans JA, Truscott JG, Milner R, Smith MA. *A Phantom for Quantitative Ultrasound of Trabecular Bone*. Vol 39.; 1994.

45. Hale GM, Querry MR. Optical Constants of Water in the 200-nm to 200-μm Wavelength Region. *Appl Opt*. 1973;12(3):555. doi:10.1364/ao.12.000555

46. Hassan CM, Peppas NA. Structure and applications of poly(vinyl alcohol) hydrogels produced by conventional crosslinking or by freezing/thawing methods. *Adv Polym*

Sci. 2000;153:37-65. doi:10.1007/3-540-46414-x_2

47. Mori Y, Tokura H, Yoshikawa M. Properties of hydrogels synthesized by freezing and thawing aqueous polyvinyl alcohol solutions and their applications. *J Mater Sci*. 1997;32(2):491-496. doi:10.1023/A:1018586307534

48. Wan WK, Campbell G, Zhang ZF, Hui AJ, Boughner DR. Optimizing the tensile properties of polyvinyl alcohol hydrogel for the construction of a bioprosthetic heart valve stent. *J Biomed Mater Res*. 2002;63(6):854-861. doi:10.1002/jbm.10333

49. Pazos V, Mongrain R, Tardif JC. Polyvinyl alcohol cryogel: Optimizing the parameters of cryogenic treatment using hyperelastic models. *J Mech Behav Biomed Mater*. 2009;2(5):542-549. doi:10.1016/j.jmbbm.2009.01.003

50. Devi CU, Vasu RM, Sood AK. Design, fabrication, and characterization of a tissue-equivalent phantom for optical elastography. *J Biomed Opt*. 2005;10(4):044020. doi:10.1117/1.2003833

51. Andersson-Engels S, Berg R, Svanberg S. Effects of optical constants on time-gated transillumination of tissue and tissue-like media. *J Photochem Photobiol B Biol*. 1992;16(2):155-167. doi:10.1016/1011-1344(92)80006-H

52. Pogue BW, Patterson MS, Jiang H, Paulsen KD. Initial assessment of a simple system for frequency domain diffuse optical tomography. *Phys Med Biol*. 1995;40(10):1709-1729. doi:10.1088/0031-9155/40/10/011

53. Cubeddu R, Pifferi A, Taroni P, Torricelli A, Valentini G. Time-resolved imaging on a realistic tissue phantom: μs′ and μa images versus time-integrated images. *Appl Opt*. 1996;35(22):4533. doi:10.1364/ao.35.004533

54. Grosenick D, Hagen A, Steinkellner O, et al. A multichannel time-domain scanning fluorescence mammograph: Performance assessment and first in vivo results. *Rev Sci Instrum*. 2011;82(2). doi:10.1063/1.3543820

55. Del Bianco S, Martelli F, Cignini F, et al. Liquid phantom for investigating light propagation through layered diffusive media. *Opt Express*. 2004;12(10):2102. doi:10.1364/opex.12.002102

56. Hunter RJ, Patterson MS, Farrell TJ, Hayward JE. Haemoglobin oxygenation of a two-layer tissue-simulating phantom from time-resolved reflectance: effect of top layer thickness. *Phys Med Biol*. 2002;47(2):193-208. doi:10.1088/0031-9155/47/2/302

57. Selb J, Joseph DK, Boas DA. Time-gated optical system for depth-resolved functional brain imaging. *J Biomed Opt*. 2006;11(4):044008. doi:10.1117/1.2337320

58. Milej D, Kacprzak M, Zołek N, et al. Advantages of fluorescence over diffuse reflectance measurements tested in phantom experiments with dynamic inflow of ICG. *Opto-electronics Rev*. 2010;18(2):208-213. doi:10.2478/s11772-010-0013-z

59. Martelli F, Pifferi A, Contini D, et al. Phantoms for diffuse optical imaging based on totally absorbing objects, part 1: basic concepts. *J Biomed Opt*. 2013;18(6):066014. doi:10.1117/1.jbo.18.6.066014

60. Martelli F, Ninni P Di, Zaccanti G, et al. Phantoms for diffuse optical imaging based on totally absorbing objects, part 2: experimental implementation. *J Biomed Opt*. 2014;19(7):076011. doi:10.1117/1.jbo.19.7.076011

61. Gibson A, Yusof RM, Dehghani H, et al. Optical tomography of a realistic neonatal head phantom. *Appl Opt*. 2003;42(16):3109. doi:10.1364/ao.42.003109

62. Grosenick D, Kummrow A, MacDonald R, Schlag PM, Rinneberg H. Evaluation of

higher-order time-domain perturbation theory of photon diffusion on breast-equivalent phantoms and optical mammograms. *Phys Rev E - Stat Nonlinear, Soft Matter Phys*. 2007;76(6):061908. doi:10.1103/PhysRevE.76.061908

63. Cubeddu R, Pifferi A, Taroni P, Torricelli A, Valentini G. A solid tissue phantom for photon migration studies. *Phys Med Biol*. 1997;42(10):1971-1979. doi:10.1088/0031-9155/42/10/011

64. Pardini P, Pomarico J, Iriarte D. A novelty technique for the fabrication of biomedical optics phantoms with cyst-mimicking inclusions. *J Near Infrared Spectrosc*. 2017;25(2):91-102. doi:10.1177/0967033516686045

65. Afshari A, Ghassemi P, Lin J, et al. Cerebral oximetry performance testing with a 3D-printed vascular array phantom. *Biomed Opt Express*. 2019;10(8):3731. doi:10.1364/boe.10.003731

66. Gehrung M, Bohndiek SE, Brunker J. Development of a blood oxygenation phantom for photoacoustic tomography combined with online pO2 detection and flow spectrometry. *J Biomed Opt*. 2019;24(12):1. doi:10.1117/1.JBO.24.12.121908

67. Kleiser S, Nasseri N, Andresen B, Greisen G, Wolf M. Comparison of tissue oximeters on a liquid phantom with adjustable optical properties. *Biomed Opt Express*. 2016;7(8):2973. doi:10.1364/boe.7.002973

68. Nasseri N, Kleiser S, Ostojic D, Karen T, Wolf M. Quantifying the effect of adipose tissue in muscle oximetry by near infrared spectroscopy. *Biomed Opt Express*. 2016;7(11):4605. doi:10.1364/boe.7.004605

69. Franceschini MA, Fantini S, Paunescu LA, Maier JS, Gratton E. Influence of a superficial layer in the quantitative spectroscopic study of strongly scattering media. *Appl Opt*. 1998;37(31):7447. doi:10.1364/ao.37.007447

70. Bisaillon C-É, Dufour ML, Lamouche G. Artery phantoms for intravascular optical coherence tomography: healthy arteries. *Biomed Opt Express*. 2011;2(9):2599. doi:10.1364/boe.2.002599

71. Elvira L, Durán C, Higuti RT, et al. Development and Characterization of Medical Phantoms for Ultrasound Imaging Based on Customizable and Mouldable Polyvinyl Alcohol Cryogel–Based Materials and 3-D Printing: Application to High-Frequency Cranial Ultrasonography in Infants. *Ultrasound Med Biol*. 2019;45(8):2226-2241. doi:10.1016/j.ultrasmedbio.2019.04.030

72. Koh PH, Elwell CE, Delpy DT. Development of a dynamic test phantom for optical topography. In: *Advances in Experimental Medicine and Biology*. Vol 645. Springer, Boston, MA; 2009:141-146. doi:10.1007/978-0-387-85998-9_22

73. Hebden JC, Brunker J, Correia T, Price BD, Gibson AP, Everdell NL. An electrically-activated dynamic tissue-equivalent phantom for assessment of diffuse optical imaging systems. *Phys Med Biol*. 2008;53(2):329-337. doi:10.1088/0031-9155/53/2/002

74. Hebden JC, Correia T, Khakoo I, Gibson AP, Everdell NL. A dynamic optical imaging phantom based on an array of semiconductor diodes. *Phys Med Biol*. 2008;53(21):N407-N413. doi:10.1088/0031-9155/53/21/N01

75. Correia T, Banga A, Everdell NL, Gibson AP, Hebden JC. A quantitative assessment of the depth sensitivity of an optical topography system using a solid dynamic tissue-phantom. *Phys Med Biol*. 2009;54(20):6277-6286. doi:10.1088/0031-9155/54/20/016

76. Funane T, Atsumori H, Kiguchi M, Tanikawa Y, Okada E. Dynamic phantom with two stage-driven absorbers for mimicking hemoglobin changes in superficial and deep tissues. *J Biomed Opt*. 2012;17(4):047001. doi:10.1117/1.jbo.17.4.047001

77. Pifferi A, Torricelli A, Cubeddu R, et al. Mechanically switchable solid inhomogeneous phantom for performance tests in diffuse imaging and spectroscopy. *J Biomed Opt*. 2015;20(12):121304. doi:10.1117/1.jbo.20.12.121304

78. Kawaguchi H, Tanikawa Y, Yamada T. Design and fabrication of a multi-layered solid dynamic phantom: validation platform on methods for reducing scalp-hemodynamic effect from fNIRS signal. In: Tromberg BJ, Yodh AG, Sevick-Muraca EM, Alfano RR, eds. *Optical Tomography and Spectroscopy of Tissue XII*. Vol 10059. SPIE; 2017:1005925. doi:10.1117/12.2250485

79. Kim H, Hau NT, Chae Y-G, Lee B, Kang HW. 3D printing-assisted fabrication of double-layered optical tissue phantoms for laser tattoo treatments. *Lasers Surg Med*. 2016;48(4):392-399. doi:10.1002/lsm.22469

80. Li J, Wu C, Chu PK, Gelinsky M. 3D printing of hydrogels: Rational design strategies and emerging biomedical applications. *Mater Sci Eng R Reports*. 2020;140:100543. doi:10.1016/j.mser.2020.100543

81. Ma C, Shen S, Liu G, et al. Multimodal 3d printing of phantoms to simulate biological tissue. *J Vis Exp*. 2019;2020(155):60563. doi:10.3791/60563

82. Diep P, Pannem S, Sweer J, et al. Three-dimensional printed optical phantoms with customized absorption and scattering properties. *Biomed Opt Express*. 2015;6(11):4212. doi:10.1364/boe.6.004212

83. Nguyen TTA, Le HND, Vo M, Wang Z, Luu L, Ramella-Roman JC. Three-dimensional phantoms for curvature correction in spatial frequency domain imaging. *Biomed Opt Express*. 2012;3(6):1200. doi:10.1364/boe.3.001200

84. Lurie KL, Smith GT, Khan SA, Liao JC, Ellerbee AK. Three-dimensional, distendable bladder phantom for optical coherence tomography and white light cystoscopy. *J Biomed Opt*. 2014;19(3):036009. doi:10.1117/1.jbo.19.3.036009

85. Stohanzlova P, Kolar R. Tissue perfusion modelling in optical coherence tomography. *Biomed Eng Online*. 2017;16(1):27. doi:10.1186/s12938-017-0320-4

86. Corcoran A, Muyo G, Van Hemert J, Gorman A, Harvey AR. Application of a wide-field phantom eye for optical coherence tomography and reflectance imaging. *J Mod Opt*. 2015;62(21):1828-1838. doi:10.1080/09500340.2015.1045309

87. Ruiz AJ, Wu M, LaRochelle EPM, et al. Indocyanine green matching phantom for fluorescence-guided surgery imaging system characterization and performance assessment. *J Biomed Opt*. 2020;25(05):1. doi:10.1117/1.JBO.25.5.056003

88. Aycock KI, Hariharan P, Craven BA. Particle image velocimetry measurements in an anatomical vascular model fabricated using inkjet 3D printing. *Exp Fluids*. 2017;58(11):1-8. doi:10.1007/s00348-017-2403-1

89. Liu Y, Ghassemi P, Depkon A, et al. Biomimetic 3D-printed neurovascular phantoms for near-infrared fluorescence imaging. *Biomed Opt Express.* 2018;9(6):2810. doi:10.1364/boe.9.002810

90. Bentz BZ, Bowen AG, Lin D, et al. Printed optics: phantoms for quantitative deep tissue fluorescence imaging. *Opt Lett*. 2016;41(22):5230. doi:10.1364/ol.41.005230

91. Ghassemi P, Wang J, Melchiorri AJ, et al. Rapid prototyping of biomimetic vascular phantoms for hyperspectral reflectance imaging. *J Biomed Opt*. 2015;20(12):121312. doi:10.1117/1.JBO.20.12.121312

92. Dempsey LA, Persad M, Powell S, Chitnis D, Hebden JC. Geometrically complex 3D-printed phantoms for diffuse optical imaging. *Biomed Opt Express*. 2017;8(3):1754.

doi:10.1364/boe.8.001754

93. Ho WH, Tshimanga IJ, Ngoepe MN, Jermy MC, Geoghegan PH. Evaluation of a Desktop 3D Printed Rigid Refractive-Indexed-Matched Flow Phantom for PIV Measurements on Cerebral Aneurysms. *Cardiovasc Eng Technol*. 2020;11(1):14-23. doi:10.1007/s13239-019-00444-z